AppliedChem

MDPI

Article

Antibacterial and Antivirulence Activity of Lyophilized *Plumbago auriculata* Flower Extract Against *Escherichia coli* and *Proteus mirabilis*

Alejandra Villarreal Araujo [1], Macdiel Acevedo Quiroz [2], Brenda Escamilla Sánchez [1], Verónica Martínez-Santos [3], Mónica Ramírez [3], Ricardo Salazar [3], Ma. Elena Moreno Godínez [1], Yaneth Castro Coronel [1], Daniel Tapia Maruri [4], Manasés González Cortazar [5], Natividad Castro Alarcón [1] and Patricia Alvarez Fitz [3,*]

[1] Faculty of Chemical and Biological Science, Autonomous University of Guerrero, Av. Lázaro Cárdenas s/n, Ciudad Universitaria Sur, La Haciendita, Chilpancingo 39090, Mexico; villarreal_ava_araujo@outlook.com or 10134518@uagro.mx (A.V.A.); 16265929@uagro.mx (B.E.S.); 11596@uagro.mx (M.E.M.G.); 12929@uagro.mx (Y.C.C.); natividadcastro@uagro.mx (N.C.A.)
[2] Department of Chemistry and Biochemistry, National Institute of Technology of Mexico, Calzada Tecnológico 27, Zacatepec de Hidalgo 62780, Mexico; macdiel.acevedoqui@uaem.mx
[3] SECIHTI, Autonomous University of Guerrero, Av. Javier Méndez Aponte No. 1, Fracc. Servidor Agrario, Chilpancingo 39070, Mexico; vimartinez@secihti.mx (V.M.-S.); mramirezru@secihti.mx (M.R.); rsalazarlo@secihti.mx (R.S.)
[4] Department od Advanced Microscopy, CEPROBI, Biotic Products Development Center, Ctra. Yautepec-Jojutla, Calle CEPROBI 8, Yautepec 62739, Mexico; dmaruri@ipn.mx
[5] Department of Phytochemical, Southern Biomedical Research Center IMSS, República de Argentina 1, Col. Centro, Xochitepec 62790, Mexico; manases.gonzalez@imss.gob.mx or gmanases2000@gmail.com
* Correspondence: paty_fitz@hotmail.com or palvarezfi@secihti.mx; Tel.: +52-7771069178

Abstract

Medicinal plants are recognized for their rich bioactive compounds, offering significant potential in the development of therapeutic alternatives to address current public health challenges. *Plumbago auriculata* is a traditionally used plant with the potential to treat various conditions. Therefore, this study evaluated the physicochemical properties and antibacterial and antivirulence potential of the lyophilized extract from *Plumbago auriculata* (ELPa). Physicochemical analysis revealed a highly porous morphology (pore diameter 5–10 μm), a yellowish-green color (Hue angle of 182.92), and a water activity (a_w) of 0.5. Antibacterial assays established a minimum inhibitory concentration (MIC) of 64 mg/mL for clinical isolates of *Escherichia coli* (*E. coli*), *Staphylococcus sciuri* (*S. sciuri*), *Staphylococcus aureus* (*S. aureus*), *Candida tropicalis* (*C. tropicalis*), *Streptococcus agalactiae* (*S. agalactiae*), and *Salmonella Dublin* (*S. Dublin*) and 16 mg/mL for the *E. coli* CFT073 strain. Furthermore, ELPa demonstrated significant antivirulence properties; at a concentration of 8 mg/mL, the extract inhibited 55% of the swarming mobility and 58% of biofilm production in *E. coli* CFT073 after 24 and 48 h of exposure, respectively. The finding suggests that ELPa is a viable source of bioactive compounds with both antibacterial and antivirulence capabilities.

Keywords: *Plumbago auriculata*; *Escherichia coli*; swarming; antibacterial; lyophilization; biofilm

Check for updates

Academic Editor: Dimitrios-Rafail Kalompatsios

Received: 21 March 2026
Revised: 29 April 2026
Accepted: 29 April 2026
Published: 9 May 2026

Copyright: © 2026 by the authors. Licensee MDPI, Basel, Switzerland. This article is an open access article distributed under the terms and conditions of the Creative Commons Attribution (CC BY) license.

1. Introduction

Infectious diseases are a major cause of morbidity and mortality. The World Health Organization (WHO) reports that six of the ten most important threats to global public health are directly related to diseases, especially those caused by multi-resistant bacteria.

Additionally, the WHO warns that the end of the antibiotic era is approaching, as antimicrobial resistance threatens to reach a point where infections cannot be easily treated [1,2]. This problem is more pronounced in countries such as Mexico, where more than 700 thousand deaths are reported annually [3]. The search for drugs targeting virulence factors offers a new approach to antibacterial therapies, aiming to suppress the production of factors essential to bacterial pathogenicity and thus prevent the development of drug resistance [4]. The global action plans proposed by the WHO (Plan for the Prevention and Control of Non-Communicable Diseases 2013–2030 and Global Action Plan on Antimicrobial Resistance) support urgent investment in the development of new drugs, diagnostics, and vaccines, among others.

Plants could represent a feasible strategy used in traditional medicine to address various health conditions, including bacterial infections. It is estimated that around 80% of the world's population uses plants as a primary treatment for other health conditions. It has been widely documented that their biological properties are due to the broad spectrum of their bioactive compounds [5].

The genus *Plumbago* comprises 280 species in the Plumbaginaceae family, native to warm temperate to tropical regions of the world, and used worldwide. It includes perennial shrubs or herbs, and the hairy calyx is a characteristic feature of the genus, associated with insect capture among other functions. *Plumbago* is the largest genus in the family. In southern Africa, five species are native, and two are cultivated. The species are grown and used worldwide mainly for their medicinal and biological properties, attributed to their chemical components [6,7]. The most cultivated species of the genus *Plumbago* are *Plumbago indica*, *Plumbago rosea*, *Plumbago zeylanica*, and *Plumbago auriculata* (*P. auriculata*) [8,9].

One of the most representative species of the genus is *Plumbago auriculata*, popularly known as "Blue Jasmine". Traditionally, the powdered root has been used to treat a wide range of diseases, including wounds, broken bones, and headaches. Although it is endemic to South Africa, it is well-adapted in Mexico and is known as a house and ornamental plant [10]. For this species, only floristic studies have been reported; antibacterial, anti-inflammatory, antioxidant, antigenotoxic, and antiproliferative activities of polar extracts have been reported, and phytochemicals such as saponins, terpenes, flavonoids, and coumarins were identified [11,12].

An interesting fact is the limited information on the use of aqueous extracts, which are highly sensitive to environmental factors, including light, heat, pH, oxygen exposure, and the presence of oxidative enzymes [13]. In this context, freeze-drying is a technique that offers an alternative for handling sensitive substances, preventing compounds from undergoing adverse reactions, and consequently from losing biological activity [14].

By optimally preserving the structural properties of plant extracts, freeze-drying becomes a key tool for ensuring the stability and efficacy of bioactive compounds. This is especially relevant in the context of the global increase in bacterial diseases, where the use of natural resources, such as *P. auriculata*, offers promising alternatives for developing new treatments.

One of the Gram-negative bacteria that constitutes a public health problem worldwide is *Proteus mirabilis* (*P. mirabilis*). It has a rod-shaped morphology, is well-known for its urease production, and its exhibits a distinctive ability to differentiate into elongated swarmer cells and a characteristic mobility pattern in the form of concentric halos on agar plates. *P. mirabilis* belongs to the class *Gammaproteobacteria* and has long been recognized as a member of the order *Enterobacteriales* [15]. In addition, within this family is *Escherichia coli* (*E. coli*), a Gram-negative bacterium previously classified within the order *Enterobacteriales*. It is recognized as a common cause of urinary tract infections (including kidney infections), sepsis, and diarrhea. The combination of virulence factors and the ability to form biofilms

makes *E. coli* a highly versatile and resistant pathogen, especially in hospital settings. Its ability to adhere to tissues, evade immune responses, and survive in communities protected by biofilms represents a significant challenge in the treatment of associated infections. This knowledge underscores the need to develop targeted therapeutic strategies that address both the virulence and the biofilm of *E. coli* [16]. Based on the above, the objective of this work was to determine the physicochemical properties and the antibacterial and antivirulence activities of lyophilized extracts from *P. auriculata* against strains of clinically important bacteria.

2. Materials and Methods

2.1. Materials and Reagents

Trifluoroacetic acid (HPLC grade), acetonitrile (HPLC grade), 3-(4,5-dimethylthiazol-2-yl)-2,5-diphenyltetrazole bromide (MTT), and the Supelco® (Bellefonte, PA, USA) C18 column were obtained from Sigma-Aldrich, Merck (Darmstadt, Germany). Mueller-Hinton broth and Mueller-Hinton agar were obtained from DIFCO Becton Dickinson and company (7 Loveton Circle, Sparks, MD, USA). The antibiotic amikacin 500 mg/2 mL solution for injection was obtained from Pharmaceutical Marketing Company of Chiapas S.A.P.I of C.V. Glycerol, glucose, glacial acetic acid, and crystal violet were obtained from J.T. Baker (Mallinckrodt Baker S.A. de C.V. Xalostoc, Edo de Mex). The solvents hexane and methanol were obtained from Golden Bell (Cuenca #63, Col Alamos, Del. Benito Juarez CDMX). The bacterial strains were provided by the Microbiology Laboratory of UAGro. The flowers of *P. auriculata* were collected at the Autonomous University of Guerrero Botanical Garden.

2.2. Plant Material

Flowers of *P. auriculata* were collected at the Autonomous University of Guerrero (UAGRO) Botanical Garden in November 2024. Herbarium specimens were prepared for deposition at the UAGro Herbarium and authenticated by M. C. Francisco S. Maradiaga Ceceña. Taxonomic identification confirmed that the specimens were *Plumbago auriculata*, commonly known as blue jasmine. The voucher number assigned was EscamillaB-006FCQB.

2.3. Preparation and Lyophilization of the Aqueous Extract

To obtain the aqueous extract (EA), the flowers were cleaned and cut into small pieces. The plant material underwent solid–liquid extraction by the infusion technique [17]. Fresh plant material was placed in hot distilled water (60 °C) for 4 h. The EA was then filtered, frozen at −20 °C, and stored in the dark until lyophilization. To obtain the freeze-dried extract of *P. auriculata* (ELPa), frozen samples were freeze-dried following the established protocol [18] using a FreeZone 4.5 L freeze dryer (Labconco, Kansas, MO, USA) with the vacuum chamber set to 12 kPa and a temperature of −50 °C. The lyophilized samples were stored at room temperature in Falcon tubes (50 mL) protected from light. The percentage yield of the lyophilized extract was calculated using Equation (1).

$$\% \text{ yield} = \frac{(g)\ of\ the\ lyophilized\ extract\ obtained}{(g)\ of\ the\ plant\ material} \times 100 \quad (1)$$

2.4. Preliminary Phytochemical Profiles by HPLC and GC-MS of the ELPa

Two fractions were obtained from the lyophilized samples: an aqueous (polar) fraction and a hexane (nonpolar) fraction. The aqueous fraction was chromatographically analyzed for ELPa using a Supelco® C18 column (250 × 4.6 mm internal diameter, 5 µm particle size (Sigma-Aldrich)). The mobile phase consisted of a 0.5% aqueous solution of trifluoroacetic acid (solvent A) and acetonitrile (solvent B). The following gradient was used: 0–1 min, 0% B; 2–3 min, 5% B; 4–20 min, 30% B; 21–23 min, 50% B; 24–25 min, 80% B; 26–27 min,

100% B; 28–30 min, 0% B. The flow rate was maintained at 0.9 mL/min, and the injection volume was 10 µL. Absorbance was measured at 330 and 280 nm. A preliminary identification of resolved peaks was performed by comparing their characteristic bands and retention times with those of known compounds [19].

Gas chromatography-mass spectrometry (GC-MS) analysis of the hexane fraction was performed as described by Sánchez-Valdeolivar et al. (2020) [20]. Samples were analyzed in triplicate using an Agilent 6890 series gas chromatograph equipped with a 5973N mass selective detector (Agilent Technologies, Inc., Santa Clara, CA, USA). The experimental conditions of the GC-MS system were as follows: HP-5MS nonpolar capillary column (30 m, ID: 0.20 mm, film thickness: 0.25 µm). The carrier gas was helium at a flow rate of 1.0 mL/min. In gas chromatography, the oven temperature program was 50 °C, increasing to 230 °C at 2 °C/min. The injection volume was 1 µL. Samples were dissolved in hexane. All results were compared using the NIST/EPA/NIH mass spectral library version 1.7a/ChemStation.

2.5. Microstructure of the ELPa

The ELPa microstructure was characterized using environmental scanning electron microscopy (ESEM), following the methodology described by Delgado et al. (2020) [21] with some modifications. The ELPa was placed on aluminum supports secured with double-sided copper conductive tape and directly analyzed using an environmental scanning electron microscope (Carl Zeiss, EVO LS10, Munich, Germany). Operating conditions included an accelerating voltage of 30 kV and a water vapor pressure of 40 Pa. For image acquisition, a backscattered electron detector (NTS BSD) was used. Images were captured in grayscale and stored as TIFFs at 1024 × 768 pixels for later analysis.

2.6. Physicochemical Analysis of the Color and a_w of the ELPa

The color analysis of ELPa was performed following the procedure described by Li et al. (2021) [22] using a CI62 X-Rite Spectrocolorimeter (X-Rite, Grandville, MI, USA). The CIELAB parameters were determined: L* (Lightness, range 0 (darkest) to 100 (brightest)), a* (reddish-greenish), and b* (yellowish-blue). From these values, chroma values (C* = $\sqrt{b^{*2} + a^{*2}}$ and the hue angle (Hue) °H = 180 + (Arc Tan (b*/a*)) were calculated using the corresponding equations.

The water activity (a_w) of ELPa was assessed following the established protocol [23], using the AquaLab electronic water activity system (Aqualab Dew Point 4TEV, Medstead, UK) at 25 °C.

2.7. Antibacterial Activity

2.7.1. Bacterial Strains

The microorganisms used in this investigation were clinical isolates of *Proteus mirabilis* 884, *Escherichia coli* CFTO73, *E. coli* IEC-181-2, *E. coli* clinical isolate, *Salmonella Dublin* 9676, *Staphylococcus sciuri* 2996, *Staphylococcus aureus* 923, *C. tropicalis*, and *S. agalactiae*, provided by the Microbiology Laboratory of UAGro. The bacterial strains were preserved at −80 °C in cryovials containing Mueller-Hinton broth (MH broth) and glycerol (30% *v*/*v*). Before use, the bacterial strains were activated (37 °C for 24 h) in MH broth. The inoculum for the assay was prepared by suspending colonies directly in Mueller-Hinton agar and adjusting the suspension to a McFarland 0.5 standard. Amikacin was used as the positive control.

2.7.2. Determination of Minimum Inhibitory Concentrations of ELPa

The minimum inhibitory concentration (MIC) of ELPa was determined by the broth microdilution method, following the standards of the Clinical and Laboratory Standards Institute (CLSI) [24] with some modifications. Amikacin (100 µg/mL) was used as a positive

control. Briefly, after preparing a stock solution of ELPa, we performed twofold serial dilutions (4–64 mg/mL) in a sterile 96-well plate containing MH broth (100 µL). We then inoculated the wells with 3 µL of the bacterial inoculum suspension (4.5×10^4 CFU/mL) and incubated them at 35 °C for 24 h. Finally, 30 µL of 3-(4,5-dimethylthiazol-2-yl)-2,5-diphenyltetrazole bromide (MTT) was added to assess metabolic activity. The MIC was defined as the lowest concentration that inhibited visible bacterial growth.

2.8. Antivirulence Activity

2.8.1. Effect of Amikacin and ELPa on Swarming Mobility

Amikacin (AMK) is proposed as a control antibiotic to determine the concentration at which it affects swarming mobility in the four clinical isolates: *P. mirabilis* 884, *E. coli* IEC-181-2, *E. coli* CFT073, and an *E. coli* clinical isolate. AMK was tested below the CLSI cutoff point (16 µg/mL) at 1.5, 0.75, 0.37, 0.18, and 0.09 µg/mL (sub-MIC concentrations). These concentrations were prepared in MH agar supplemented with 1.5% glucose prior to inoculating the plates with the strains. Plates were incubated overnight at 37 °C, after which the cultures were examined to determine the effect of each concentration on growth and swarming mobility [25].

To determine whether ELPa affects the swarming mobility of clinical isolates of *Proteus mirabilis* 884, *E. coli*, *E. coli IEC* 181-2, and *E. coli* CFT073, the diffusion technique described by Panayi et al. (2022) [26] was used, with some modifications. Strains from a 24 h culture at 37 °C on MH agar (DIFCO Becton Dickinson)) were used for this study. ELPa was dissolved in 1000 µL of sterile water, and concentrations of 4, 8, 16, 32, and 64 mg/mL were added to Petri dishes containing MH agar with 1.5% glucose. Once the agar had solidified, 5 µL of the bacterial suspension of the clinical *E. coli* isolates *E. coli* IEC 181-2 and *E. coli* CFT073 (7.5×10^5 CFU) was inoculated in the center of the dish. The dishes were incubated at 37 °C, with readings taken at 24, 48, and 72 h. AMK (0.37 µg/mL) was used as a positive control, and Mueller-Hinton agar with 1.5% glucose, without extracts, was used as a negative control. The diameter of the mobility zone was measured with a digital vernier (Proconso, Monterrey, México), and the percentage of inhibition of swarming mobility was calculated using Equation (2).

$$\% \text{ Swarming mobility inhibition} = [1 - (\text{treatment diameter}/\text{control diameter})] \times 100 \quad (2)$$

2.8.2. Effect of ELPa on Initial Biofilm Inhibition

The effect of ELPa on biofilm formation by clinical isolates of *Proteus mirabilis* 884, *E. coli*, *E. coli* IEC 181-2, and *E. coli* CFT073 was assessed according to the established protocol [5]. Strains from a 24 h culture at 37 °C on MH agar (DIFCO Becton Dickinson) were used in this study. ELPa concentrations of 4, 8, and 16 mg/mL were added to each well of a 96-well plate (Costar, Corning, NY, USA). Subsequently, 100 µL of inoculum (1×10^8 CFU/mL) was added to the wells. The 96-well plates were incubated for 48 h at 37 °C. The contents of each well were washed with 200 µL of saline solution and fixed with 200 µL of methanol for 15 min. The plates were then air-dried and stained with 200 µL of crystal violet (1%). The crystal violet was removed, and 200 µL of glacial acetic acid (33%, *v*/*v*) was added to the wells. Finally, a microplate reader (Multiskan Fc, Thermo Scientific, Waltham, MA, USA) was used to measure absorbance at 540 nm. The percentage of biofilm inhibition was calculated using Equation (3).

$$\% \text{ Biofilm inhibition} = [1 - (\text{treatment absorbance}/\text{control absorbance})] \times 100 \quad (3)$$

2.9. Statistical Analysis

Data are presented as the mean (±standard deviation) across three experiments conducted at independent times. Statistical analysis was performed using one-way ANOVA with a Dunnett post hoc test using GraphPad Prism V 8.0. Results with $p < 0.05$ were considered statistically significant.

3. Results and Discussion

3.1. Preparation and Lyophilization of the Aqueous Extract

After infusion extraction of *P. auriculata* flowers, followed by lyophilization, the final yield was 0.281%.

The use of lyophilization as a method for extract concentration is key to preserving the chemical stability and bioactive composition of plant metabolites, as this process prevents thermal and oxidative degradation that can occur with conventional drying methods. Several authors have demonstrated that lyophilization enables the production of extracts with greater purity and stability, thereby preserving thermosensitive and photosensitive compounds [27].

Ibarra et al. (2017) [28] reported the percentage yield of the dried-leaf extraction of *P. auriculata* using the percolation method with methanol as the solvent. The yield was 13.89%. These variations can be attributed to factors such as the solid-to-liquid ratio, particle size of the plant material, contact time, and extraction temperature, which directly influence process efficiency. Furthermore, it is essential to note that higher yields do not necessarily imply a higher concentration of bioactive metabolites, as sugars, proteins, and other soluble non-phenolic compounds are also extracted [29].

3.2. Identification of the Preliminary Phytochemical Profiles by HPLC of the ELPa (Polar Extract)

The chromatograms of the ELPa are presented in Figure 1a. A total of 4 peaks related to flavonoid-type compounds were observed.

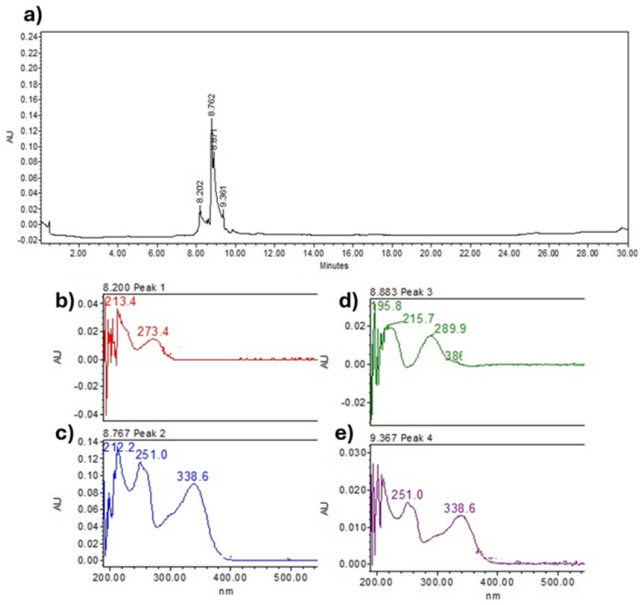


Figure 1. HPLC chromatogram of ELPa from *P. auriculata*. (**a**) Chromatogram with absorbance at 280 nm. (**b**–**e**) Broadening of the absorption bands of Peaks 1–4.

As shown in Figure 1, the peaks in the chromatograms exhibited retention times (t_R) ranging from 8.202 to 9.367 min. Based on the t_R and the absorption bands in the UV–Vis spectra (Figure 1a–e) of the peaks shown in Table 1, a preliminary analysis of the metabolites

present in the ELPa was performed by comparing these parameters with known standards and the literature data.

Table 1. Preliminary phytochemical profile by HPLC-UV–Vis analysis of ELPa.

Peak	Retention Time (min)	Absorption Bands (nm)	Compound Affinity	Refs.
1	8.202	213.4, 273.4	Coumaric acid	[7,30]
2	8.762	212.2, 251.0, 338.6	Lignan	[29]
3	8.883	95.8, 215.7, 289.9	Vanillin/Rutin	[7,30]
4	9.367	251.0, 338.6	Quercetin 3-O-glucoside	[30,31]

Accordingly, for Peak 1 (Figure 1b), the observed absorption bands at 213.4 and 273.4 nm were identical to those of coumaric acid (Figure 2a). For Peak 2 (Figure 1c), the observed absorption bands at 212.2, 251 and 338.6 nm, together with analysis of the UV–Vis bands and the literature, suggest a link (Figure 2b). Regarding Peak 3 (Figure 1d) absorption bands at 195.8, 215.7, and 306 nm were observed, and UV–Vis analysis indicated the presence of rutin and/or vanillin (Figure 2c,d). Finally, for peak 4 (Figure 1e), based on its retention time and UV–Vis band (251 and 338.6 nm), the presence of the compound quercetin 3-O-glucoside was determined (Figure 2e).

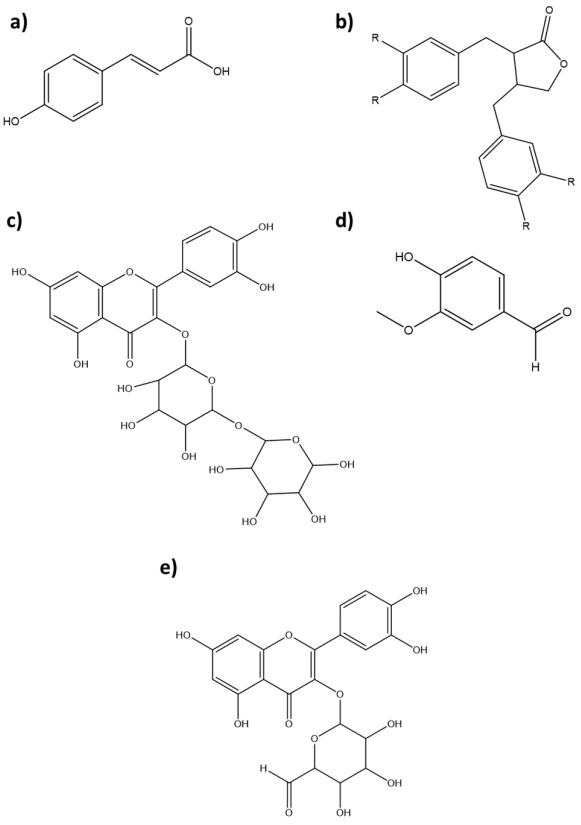


Figure 2. Chemical structures of the compounds identified in the ELPa correspond to: (**a**) coumaric acid, (**b**) lignan, (**c**) rutin, (**d**) vanillin, and (**e**) quercetin 3-O-glucoside.

To date, no reports have been found on secondary metabolites in ELPa from the flowers of *P. auriculata*. However, reports on the phytochemical composition of the alcoholic extract of the flowering aerial parts of *P. auriculata Lam*, describe the presence of sixteen compounds (gallic acid, chlorogenic acid, catechin methyl gallate, caffeic acid, syringic acid, pyrocatechol, rutin, ellagic acid, coumaric acid, vanillin, ferulic acid, naringenin, taxifolin, cinnamic acid, and kaempferol) [7]. Likewise, other studies (UPLC-MS/MS) on leaf, root,

and stem extracts (70% ethanol) from *Plumbago zeylanica* have reported the presence of hydroxyplumbagic acid, 3′-O-β-D-xylopyranosyl plumbagic acid, atractylolide, cinchonain, plumbagin, and cinchonain [30].

3.3. Chemical Profile of the Hexane Extract of Plumbago Auriculata Flower by GC-MS (Non-Polar Extract)

Analysis of the GC-MS chromatograms of the hexane extract of *P. auriculata* flowers identified six phytochemical compounds (Figure S1). Table 2 lists the detected compounds, in elution order. The most abundant compounds in the extract were decanedioic acid, dibutyl ester (73%), and heptacosane (12%), which together accounted for approximately 85% of the extract's content. Compound identification was based on peak area (%) and retention time (t_R) (Table 2).

Table 2. Chemical composition of the hexane extract of *Plumbago auriculata* using GC-MS.

Compound	Compound Name	Molecular Formula	Molecular Weight (g/mol)	Peak Area	Area (%)	Retention Time (t_R)
1	Methyl stearate	$CH_3\ (CH_2)_{16}\ CO_2\ CH_3$	298.51	116,144,899.4	7.71	18.547
2	Decanedioic acid, dibutyl ester	$C_{18}H_{34}O_4$	314.46	992,065,803.4	65.89	18.941
3	Heptyl hexacosyl ether	$C_{33}H_{68}O$	480.8924	87,082,321.55	5.78	21.81
4	9-(2′,2′-Dimethylpropanoyl-hydrazone)-3,6-dichloro-2,7-bis-[2-(diethylamino)-ethoxyfluorene	$C_{30}H_{42}Cl_2N_4O_3$	577.6	47,020,231.96	3.12	23.322
5	Nonadecane	$C_{19}H_40$	268.5	89,823,505.32	5.97	24.885
6	Heptacosane	$C_{27}H_{56}$	380.74	173,470,695.5	11.52	27.863

It is important to note that this is the first report of a GC-MS analysis of a hexane extract from *P. auriculata* flowers. However, similar studies have been documented for other species of the genus *Plumbago*. One example is the study by Hasan et al. (2023) [31], which identified compounds such as 1,3-dimethylbenzene, p-cymene, benzaldehyde, o-cymene, 5-ethyl-2-methyl-o-xylene, α-cymene, decenal, dodecane, 2,6-dimethylnaphthalene, 2,6-di-tert-butyl-1,4-benzoquinone, 2-methoxy-4-vinylphenol, eugenol, β-elemene, 2,4-di-tert-butylphenol, α-bisabolene, β-ionone, dodecanoic acid, germacrene D, 2,6-di-tert-butyl-1,4-benzenediol, 2-(1,1-dimethylethyl)phenol, 2,6-di-tert-butyl-4-ethylphenol, tetradecanoic acid, eudesmol-(1,11)-dioxo-8,12-diol, spathulenol, hexadecanoic acid, diisobutyl phthalate, piperine, hexadecanoyl-hydroxy acetone, 1,1,3-trimethyl-3-phenyl-1,3-dihydroxyindene, bromohexane, diethanolamine, tripropyl phosphate, methyl heptadecanoate, benzene-1,1′-(1,2,3-trimethylpropyl)-1,2-di amino, hexadecanoic acid, eicosane, phytol, methyl 11-octadecenoate, methyl palmitate, diethyl phthalate, eicosene, nonacosanoic acid, docosene, 2,6,10,15-tetramethyl heptadecane, tetrosene, heneicosane, diisopropyl phthalate, and octacosane from the essential oil of *P. auriculata* flowers.

3.4. Microstructure of the ELPa

Microscopic characteristics revealed agglomerates with irregular and fractured surfaces (Figure 3a). Concavities of approximately 30 μm were observed (Figure 3b). However, a detailed analysis of the ELPa microstructure revealed the presence of porous channels with rough and irregular surfaces (Figure 3c). It was also observed that the ELPa has pores with diameters ranging from 5 to 10 μm (Figure 3d). The microstructure was notable for its uniformly distributed, honeycomb-like concavities, which give the ELPa an irregular porous structure (Figure 3d).

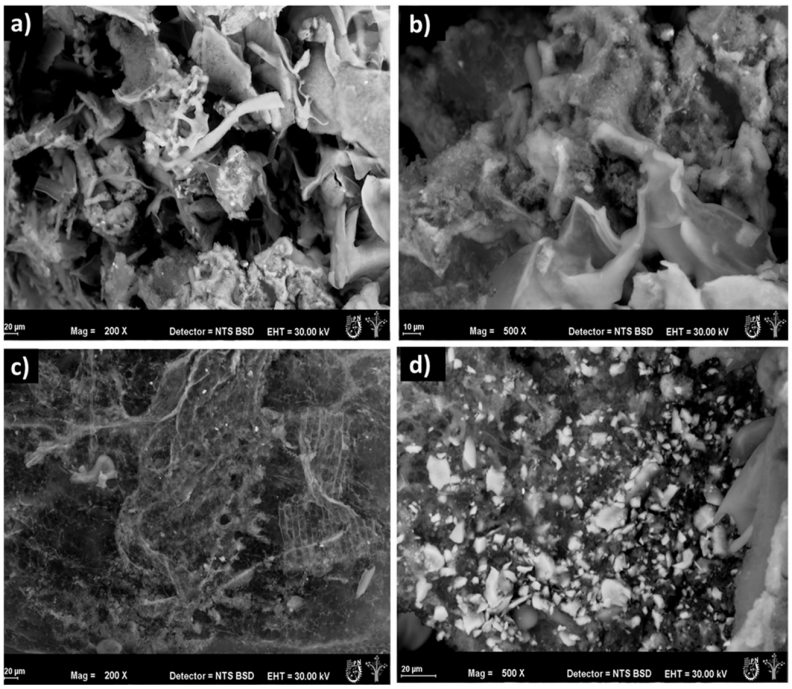


Figure 3. Scanning electron microscopy (SEM) micrographs of ELPa: (**a**) (200×), (**b**) (500×), (**c**) (500×), and (**d**) (200×).

A study by Oikonomopoulou et al. (2011) [32] demonstrated that environmental scanning electron micrographs of rice and strawberries, obtained at lower pressures during freeze-drying, showed significantly increased porosity. On the other hand, Kim et al. (2008) [33] freeze-dried on polymers such as polylactic acid, demonstrating a honeycomb-like morphology. This structural pattern results from the formation and sublimation of aligned solvent crystals during the controlled freezing stage. These crystals act as templates that direct the formation of microtubes or pores in the final material.

3.5. Physicochemical Analysis of ELPa

Determination of Color and a_w

Determining the color of an ELPa is key because it serves as an indicator of its quality, chemical composition, and stability. Color is associated with the presence of bioactive compounds such as polyphenols, flavonoids, and anthocyanins, which are sensitive to processing conditions. Color changes may reflect oxidation, thermal degradation, or loss of extract activity [34]. Additionally, colorimetric analysis of ELPa was performed using the CIE L a*b* system. It was observed that ELPa exhibited yellow tones (b*: 3.66), followed by green tones (a*: −0.796), luminosity closer to dark colors than to light ones (L of 19.168), and low saturation (C: 2.383), which, in addition to the hue angle, positioned ELPa within the green color range (°H: 182.92).

Water activity (a_w) strongly influences the growth and metabolic activity of microorganisms, as well as the rates of chemical and enzymatic reactions. It is a critical parameter for the stability and quality of lyophilized products. The ELPa had an a_w of 0.5. Notably, an aw below 0.6 inhibits the growth of bacteria, yeasts, and molds; however, as the a_w exceeds 0.6, chemical and enzymatic reactions predominate, which can affect the quality and stability of the product [23,35].

3.6. Antibacterial Activity

Minimum Inhibitory Concentration (MIC)

The MIC is the lowest concentration of an antimicrobial agent (extracts, antibiotics, purified compounds) that inhibits the growth of microbial pathogens after a 24 h incubation [35]. Results obtained for determining the MIC showed that ELPa exhibited antibacterial activity, inhibiting the growth of all strains tested (Table 3). However, the lowest MIC was 16 mg/mL for the *E. coli* CFTO73 strain, and the remaining bacteria (Gram-positive and Gram-negative) ATCC and clinical isolates presented an MIC of 64 mg/mL.

Table 3. Minimum inhibitory concentration (MIC) of ELPa.

	Bacteria	ELPa (mg/mL)
ATCC	*Staphylococcus sciuri* 29061	64
	Staphylococcus aureus 25923	64
	Escherichia coli CFT073	16
Clinical isolates	*Escherichia coli*	64
	Escherichia coli 181-2	64
	Streptococcus agalactiae 208310265	64
	Salmonella Dublin 9676	64
	Candida tropicalis	64
	Proteus mirabilis 884	64

Although there are few reports on the antibacterial activity of *P. auriculata*, there are reports on other species of the genus *Plumbago*. In this regard, Saha & Paul (2014) [36], determined the MIC of the methanolic extract of *Plumbago indica* leaves, which inhibited the growth of *Bacillus subtilis*, *Bacillus megaterium*, *Pseudomonas aeruginosa*, *Escherichia coli*, *Shigella sonnei*, and *Vibrio cholerae* at an MIC of 125 µg/mL, while for *S. aureus*, *Shigella dysentariae*, and *Salmonella paratyphi*, an MIC of 62.5 µg/mL was observed. For *Bacillus cereus* and *Salmonella typhi*, MICs of 31.25 µg/mL were observed. The results were not similar to those observed for the MIC of the ELPa, which was attributed to differences in the phytochemical composition between the two species [37]. Likewise, Khatun (2023) [38] points out that *P. indica* contains a wide range of bioactive compounds, such as alkaloids, flavonoids, saponins, glycosides, tannins, and naphthoquinones, including plumbagin. Within this range of metabolites, the compounds identified in the EA of *P. auriculata* flowers by HPLC in this study include flavonoids such as cyanidin, coumaric acid, lignans, apigenin diglucoside, rutin, and vanillin. Several authors have reported that these compounds exhibit antibacterial activity against Gram-positive and -negative bacteria [39], demonstrating that *p*-coumaric acid killed the bacteria by disrupting bacterial cell membranes and binding to bacterial genomic DNA to inhibit cellular functions. In addition, when *E. coli* is treated with anthocyanins, there is a significant increase in cell membrane permeability and growth inhibition [40]. Moreover, plumbagin impaired *E. coli* cell membrane structure and function [41].

3.7. Antivirulence Activity

Effect of Amikacin and ELPa on Swarming Mobility

Amikacin is proposed as an antibiotic to control swarming mobility. According to the CLSI, the MIC breakpoints for amikacin in *Escherichia coli* and *Proteus mirabilis* are $\leq$16 µg/mL. To determine the concentration that affects swarming mobility without affecting the growth of *P. mirabilis* and *E. coli* strains, concentrations below the breakpoint (0.09, 0.18, 0.37, 0.75, and 1.5 µg/mL) were evaluated. The results indicated that at 1.5 µg/mL, AMK completely inhibited the swarming mobility at 24 h for *E. coli* IEC-181-2 (Figure 4(A6)),

the *E. coli* clinical isolate (Figure 4(B6)), and *E. coli* CFT073 (Figure 4(C6)). However, at the same concentration for *P. mirabilis* 884, a 58.63% inhibition of the concentric halo was observed at 24 h compared to the control (Figure 4(D6)). At 0.75 µg/mL, a complete reduction in the mobility halo was still observed for the *E. coli* CFT073 strain (Figure 4(C5)).

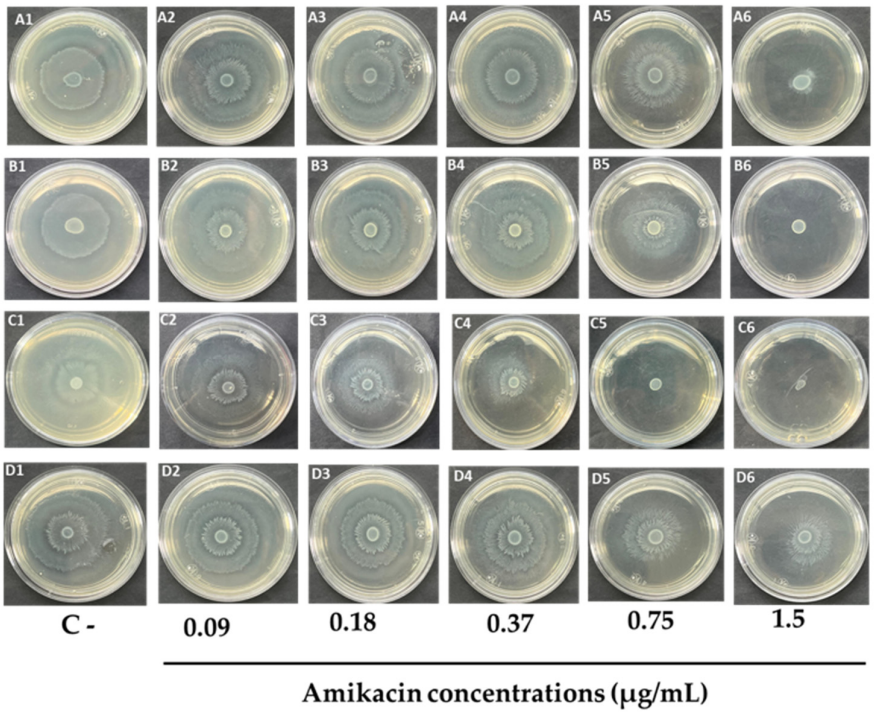


Figure 4. Effect of amikacin on swarming mobility at 24 h. Images of amikacin on the swarming mobility of (**A1**–**A6**) *E. coli* IEC-181-2; (**B1**–**B6**) clinically isolated *E. coli*; (**C1**–**C6**) *E. coli* CFT073, and (**D1**–**D6**) *P. mirabilis* 884. C−: Mueller-Hinton agar with 1.5% glucose.

Finally, it was observed that at a concentration of 0.37 µg/mL, amikacin reduced the mobility of the four selected strains without affecting growth (Figure 4(A4,B4,C4,D4)); therefore, this concentration was used as a positive control for the assays in this study.

To determine the antivirulence activity of ELPa, a swarming mobility assay was performed, as swarming mobility is essential for bacterial virulence and pathogenicity. The effect of ELPa on the swarming mobility of *P. mirabilis* 884, *E. coli* IEC 181-2, clinical isolates of *E. coli*, and *E. coli* CFT073 was evaluated. The results are shown in Table 4, and the swarming morphology at 24 h is shown in Figure 5.

Table 4. Effect of ELPa on the mobility and inhibition of swarming mobility.

Strain/ Time (h)	Concentrations (mg/mL)							
	Zone Mobility (mm)	Inhibition (%)	Zone Mobility (mm)	Inhibition (%)	Zone Mobility (mm)	Inhibition (%)	Zone Mobility (mm)	Inhibition (%)
***P. mirabilis* 884**	**C+**		**16**		**32**		**64**	
24	34.12 ± 0.13	12.10 ± 0.33	NP	100 ± 0 ****	NP	100 ± 0 ****	NP	100 ± 0 ****
48	38.02 ± 0.60	6.03 ± 1.48	NP	100 ± 0 ****	NP	100 ± 0 ****	NP	100 ± 0 ****
72	39.86 ± 0.05	5.63 ± 0.12	NP	100 ± 0 ****	NP	100 ± 0 ****	NP	100 ± 0 ****
***E. coli* CFT073**	**C+**		**4**		**8**		**16**	
24	25.32 ± 0.16	30.28 ± 0.45	28.26 ± 0.85 ****	19.80 ± 1.40	15.68 ± 0.56 ****	55.50 ± 1.6 ****	NP	100 ± 0 ****
48	33.16 ± 0.05	10.90 ± 0.14	32.92 ± 0.57 ****	9.61 ± 1.57 ****	18.66 ± 0.16 ****	48.76 ± 0.45 ****	NP	100 ± 0 ****
72	35.56 ± 0.05	7.58 ± 0.14	35.34 ± 0.48 ****	8.16 ± 1.25 ****	20.72 ± 0.16 ****	46.15 ± 0.42 ****	NP	100 ± 0 ****

Table 4. *Cont.*

Strain/ Time (h)	Concentrations (mg/mL)							
	Zone Mobility (mm)	Inhibition (%)	Zone Mobility (mm)	Inhibition (%)	Zone Mobility (mm)	Inhibition (%)	Zone Mobility (mm)	Inhibition (%)
***E. coli IEC*-181-2**	**C+**		**16**		**32**		**64**	
24	35.14 ± 0.08	13.19 ± 0.22	30.86 ± 0.47 ****	14.60 ± 1.30	26.10 ± 0.59 ****	27.78 ± 1.64 ****	NP	100 ± 0 ****
48	36.68 ± 0.08	13.0 ± 0.20	33.8 ± 0.51 ****	8.74 ± 1.38 ****	28.66 ± 0.18 ****	22.62 ± 0.49 ****	NP	100 ± 0 ****
72	39.86 ± 0.5	10.50 ± 0.12	36.54 ± 0.36 ****	7.16 ± 0.92 ****	30.74 ± 0.18 ****	21.90 ± 0.46 ****	NP	100 ± 0 ****
***E. coli* clinically isolated**	**C+**		**16**		**32**		**64**	
24	29.27 ± 0.26	8.57 ± 1.65	31.10 ± 0.1 ****	14.37 ± 0.27 ****	22.62 ± 0.29 ****	37.72 ± 0.81 ****	NP	100 ± 0 ****
48	29.30 ± 0.52	7.80 ± 1.69	35.3 ± 0.23 ****	5.15 ± 0.63 ****	28.38 ± 0.35	23.75 ± 0.95 ****	NP	100 ± 0 ****
72	29.47 ± 0.37	6.92 ± 1.03	36.38 ± 0.13 ****	4.08 ± 0.18 ****	30.82 ± 0.35 ****	19.23 ± 0.93 ****	NP	100 ± 0 ****

ELPa: lyophilized extract of *P. auriculata*. C+: positive control, Amikacin (0.37 µg/mL). The results express the mean and SD of three replicates. For the percentage of inhibition of the strains, the statistical test used was Dunnett's test compared with the positive control (C+). **** Statistically significant difference with a value of $p < 0.0001$. NP: without mobility.

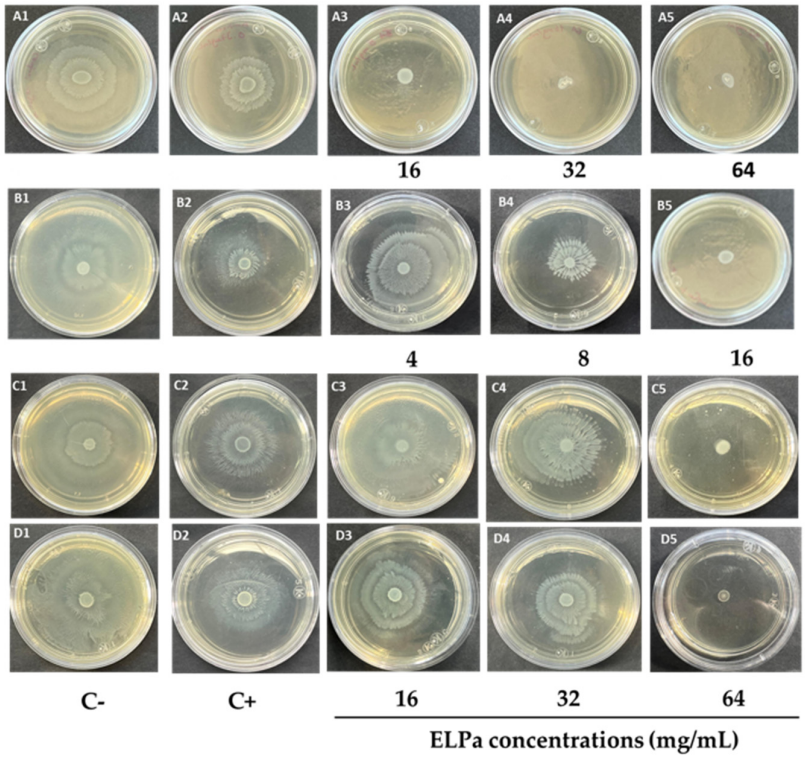


Figure 5. Representative images of ELPa on the swarming mobility of (**A1–A5**) *Proteus mirabilis* 884; (**B1–B5**) *E. coli* CFT073; (**C1–C5**) *E. coli* IEC 181-2, and (**D1–D5**) clinically isolated *E. coli*. C+: Amikacin (0.37 µg/mL); C−: Mueller-Hinton agar with 1.5% glucose inoculated with the clinical isolates at 24 h.

The *P. mirabilis* 884 strain showed high sensitivity to the ELPa extract, demonstrating a complete reduction in the swarming mobility halo (100% reduction) at concentrations of 16, 32, and 64 mg/mL (Figure 5(A3–A5), and Table 4) compared to the negative control (Figure 5(A1)) at 24 h. Likewise, for all concentrations evaluated within this range (16–64 mg/mL), 100% inhibition of swarming mobility was observed at all three exposure times analyzed compared to the negative control (Table 4).

For *E. coli* CFT073, the strain showed high sensitivity at 16 mg/mL, which completely inhibited the mobility halo formation (Figure 5(B5)) compared with the negative control (Figure 5(B1)). Across the three exposure times (24–72 h), the results showed a time-dependent relationship, with 100% inhibition maintained at 24, 48, and 72 h at

this concentration. At 24 h, the second most effective concentration was 8 mg/mL, with 55.5% inhibition; at 48 h, this decreased to 48.76%, and at 72 h, it was slightly reduced to 46.15%. Overall, at 72 h, all tested concentrations showed lower inhibitory activity than at 24 h (Table 4).

On the other hand, in the clinical isolates *E. coli* IEC-181-2 and clinically isolated *E. coli* (Figure 5(C3–C5,D3–D5)), the ELPa exhibited an effect on swarming mobility at a concentration of 32 mg/mL, with inhibition ranging from 19–37% across the three exposure times (Table 4).

To cause urinary tract infections, *E. coli* uses various virulence factors, including fimbriae, biofilm formation, swarming mobility, flagella, lipopolysaccharides, outer membrane proteins, and hemolysins. These factors are essential for enabling bacteria to colonize the urinary tract and persist despite effective host defense. Furthermore, these same virulence factors may be linked to antibiotic resistance [38]. Swarming mobility is a key process in *E. coli* pathogenicity. During this process, bacteria differentiate into a highly mobile and elongated form that enables mass migration on solid surfaces, facilitating tissue colonization and biofilm formation, thereby contributing to their virulence [42].

On the other hand, *P. mirabilis* employs various virulence factors, including urease, toxins (hemolysin, toxic agglutinin, and ZapA metalloprotease), flagella, fimbriae, and biofilm formation [43].

A study by Panayi et al. (2022) [26] evaluated ethanolic extracts of oregano and rosemary at 1 mg/mL and observed a significant inhibition of *E. coli* swarming mobility, with 54.7% and 58.3%, respectively. Furthermore, they state that swarming mobility is quorum-sensing-dependent. These extracts can be considered anti-quorum-sensing inhibitors in *E. coli* without affecting bacterial growth. They can serve as a viable alternative for treating infectious diseases caused by antibiotic-resistant pathogens.

3.8. Antivirulence Activity

Effect of ELPa on Initial Biofilm Inhibition

Therefore, the ability of ELPa to inhibit bacterial biofilm formation was evaluated at concentrations of 4, 8, and 16 mg/mL against *E. coli* IEC-181-2, a clinical isolate of *E. coli*, *P. mirabilis* 884, and *E. coli* CFT073 after 48 h of exposure. Amikacin served as the positive control, and the biofilm that formed in the absence of ELPa treatments served as the negative control.

However, the percentage inhibition results were most notable for *E. coli* CFT073 (Figure 6). At 16 mg/mL, biofilm production was inhibited 63% (<0.0001) compared with the positive control. At 8 mg/mL, inhibition was 58% (<0.0001), and at 4 mg/mL, it was 20% (<0.0001).

A bacterial biofilm is a structure composed of extracellular polymeric substances produced by one or more bacterial species that adhere to a surface. These structures confer protection by helping bacteria evade antibiotics [44].

The observed inhibitory effect on biofilm formation may be linked to bioactive compounds in *P. auriculata*, such as plumbagin. Another study by Jamal et al. (2018) [45] evaluated the antibiofilm activity of plumbagin against clinical isolates of *E. coli*. Plumbagin was effective, with minimum inhibitory concentration (MIC) values ranging from 0.029 to 0.117 µg/mL, and growth inhibition of 79% to 99% across the evaluated strains. This activity is comparable to, and in some cases superior to, conventional antibiotics such as gentamicin and vancomycin. At MIC X2 concentrations, plumbagin dramatically reduced biofilm formation, showing a significant decrease in adherent cell density in crystal violet assays. This effect is attributed to its ability to disrupt essential metabolic processes and alter gene expression associated with extracellular matrix production [46].

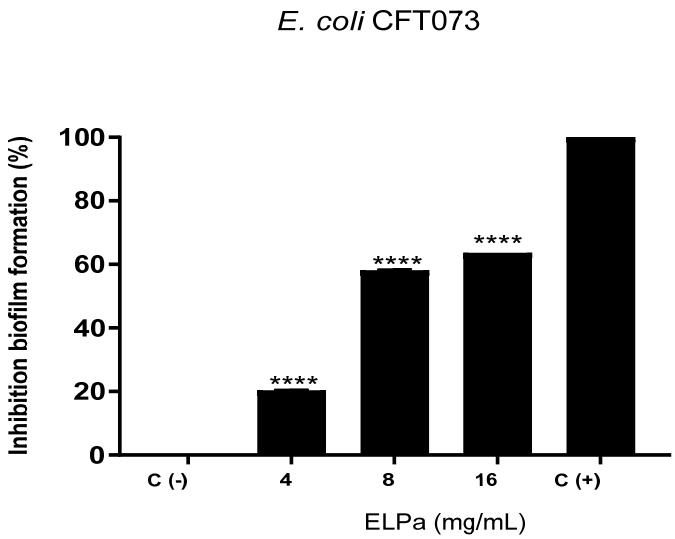


Figure 6. Percentage inhibition of biofilm formation by ELPa. C (+): positive control, Amikacin (100 µg/mL). C (−): negative control, Mueller-Hinton broth with 1.5% glucose inoculated with *E. coli* CFT073 at 48 h. The values shown represent the mean and standard deviation of three replicates. One-way ANOVA followed by Dunnett's post hoc analysis with respect to the positive control C (+). **** Statistically significant difference with a p-value < 0.0001.

4. Conclusions

This study revealed that ELPa exhibits broad-spectrum in vitro antibacterial activity against both Gram-negative and Gram-positive bacteria, including ATCC strains and clinical isolates. At sub-inhibitory concentrations (Sub-MIC), ELPa effectively inhibited swarming mobility and biofilm production in *P. mirabilis* 884, *E. coli* IEC-181-2, *E. coli* CFT073, and an *E. coli* clinical isolate. The biological activity of ELPa is supported by the preliminary identification of five polar (coumaric acid, lignan, rutin, vanillin, and quercetin 3-O-glucoside) and six non-polar compounds. However, further studies are needed to purify these constituents and unequivocally determine their biological activity, as well as to evaluate their antibacterial and antivirulence effects individually and in combination with conventional antibiotics.

Supplementary Materials: The following supplementary material can be downloaded at: https://www.mdpi.com/article/10.3390/appliedchem6020032/s1, Figure S1. GC-MS chromatograms of the hexane fraction of ELPA. (A) Peaks show retention times of the chemical compounds. (B) Spectrum of methyl stearate. (C) Decanedioic acid, dibutyl ester. (D) Heptyl hexacosyl ether. (E) 9-(2′,2′-Dimethylpropanoylhydrazone)-3,6-dichloro-2,7-bis-[2-(diethylamino)-ethoxyfluorene]. (F) Nonadecane. (G) Heptacosane.

Author Contributions: A.V.A.: Research, formal analysis, and writing (original draft). P.A.F.: Conceptualization, formal analysis, resources, and writing (review and editing). M.R.: Research and resources. M.A.Q.: Research and validation. V.M.-S.: Research and validation. B.E.S.: Research and methodology. R.S.: Methodology. Y.C.C.: Validation. N.C.A.: Validation. M.E.M.G.: Validation. D.T.M. and M.G.C.: Validation and methodology. All authors have read and agreed to the published version of the manuscript.

Funding: This research received no external funding.

Institutional Review Board Statement: Not applicable.

Informed Consent Statement: Not applicable.

Data Availability Statement: Data are contained within the article or Supplementary Materials. The original contributions presented in this study are included.

Acknowledgments: To the SECIHTI scholarship with CVU: 966924 and to Project IxM-7135-UAGro.

Conflicts of Interest: The authors declare no conflicts of interest.

References

1. World Health Organization. *World Health Statistics 2017: Monitoring Health for the SDGs, Sustainable Development Goals*; World Health Organization: Geneva, Switzerland, 2017. Available online: https://www.who.int/publications/i/item/9789241565486 (accessed on 1 October 2025).
2. World Health Organization. *World Health Statistics 2018: Monitoring Health for the SDGs, Sustainable Development Goals*; World Health Organization: Geneva, Switzerland, 2018. Available online: https://www.who.int/publications/i/item/9789241565585 (accessed on 5 October 2025).
3. Mexican Association of Infectology and Clinical Microbiology. Informe anual sobre infecciones resistentes a antibióticos en México. *Rev. Mex. Infectol. Microbiol. Clín.* **2019**, *34*, 123–130.
4. Zhao, J.; Peng, T.; Liang, S.; Ma, M.; Zeng, Z.; Yu, P.; Gong, D.; Deng, S. Antibacterial activity and action mechanism of microencapsulated dodecyl gallate with methyl-β-cyclodextrin. *Food Control* **2020**, *1*, 106–108. [CrossRef]
5. Beltrán-Martínez, M.; Tapia-Rodríguez, M.; Ayala-Zavala, J.F.; Gómez-Álvarez, A.; Robles-Zepeda, R.E.; Torres-Moreno, H.; De Rodríguez, J.; López-Romero, J.C. Antimicrobial and Antibiofilm Potential of *Flourensia retinophylla* against *Staphylococcus aureus*. *Plants* **2024**, *11*, 2632. [CrossRef]
6. Singh, K.; Naido, Y.; Baijnath, H. A comprehensive review on the genus *Plumbago* with focus on *Plumbago auriculata* (*Plumbaginaceae*). *Tradit. Complement. Altern. Med.* **2018**, *15*, 199–215. [CrossRef]
7. Melk, M.; El-Hawary, S.; Melek, F.; Saleh, D.; Ali, O.; El Raey, M.; Mohamed, N. Nano zinc oxide green-synthesized from *Plumbago auriculata* Lam. Alcoholic Extract. *Plants* **2021**, *10*, 2447. [CrossRef]
8. Yuvaraj, D.; Jalalpure, S. A comprehensive review on *Plumbago zeylanica* Linn. *Afr. J. Pharm. Pharmacol.* **2011**, *5*, 2738–2747. [CrossRef]
9. Shukla, B.; Saxena, S.; Usmani, S.; Kushwaha, P. Phytochemistry and pharmacological studies of *Plumbago zeylanica* L.: A medicinal plant review. *Clin. Phytosci.* **2021**, *1*, 2738–2747. [CrossRef]
10. Govindan, L.; Anbazhagan, S.; Altemimi, A.; Lakshminarayanan, K.; Kuppan, S.; Pratap-Singh, A.; Kandasamy, M. Efficacy of Antimicrobial and Larvicidal Activities of Green Synthesized Silver Nanoparticles Using Leaf Extract of *Plumbago auriculata* Lam. *Plants* **2020**, *9*, 1577. [CrossRef]
11. Lakshmanan, G.; Bupesh, G.; Vignesh, A.; Sathiyaseelan, A.; Murugesan, K. Micropropagation and anticancer activity of methanolic extract of *Plumbago auriculata* Lam. *Int. J. Adv. Biotechnol. Res.* **2016**, *4*, 2001–2011.
12. Thitiorul, S.; Ratanavalachai, T.; Tanuchit, S.; Itharat, S.; Sakpakdeejaroen, T. Genotoxicity and interference with cell cycle activities by an ethanolic extract from Thai *Plumbago indica* roots in human lymphocytes in vitro. *Asian Pac. J. Cancer Prev.* **2013**, *14*, 2487–2490. [CrossRef]
13. Hussain, S.; Hameed, A.; Nazir, Y.; Naz, T.; Wu, Y.; Ansar, H.; Song, Y. Microencapsulation and the characterization of polyherbal formulation (PHF) rich in natural polyphenolic compounds. *Nutrients* **2018**, *10*, 843. [CrossRef] [PubMed]
14. Borgogna, M.; Bellich, B.; Zorzin, L.; Lapasin, R.; Cesáro, A. Food microencapsulation of bioactive compounds: Rheological and thermal characterization of non-conventional gelling system. *Food Chem.* **2010**, *122*, 416–423. [CrossRef]
15. Armbruster, C.E.; Mobley, H.L.T.; Pearson, M.M. Pathogenesis of *Proteus mirabilis* Infection. *EcoSal Plus* **2018**, *8*, 10–1128. [CrossRef] [PubMed]
16. Pakbin, B.; Brück, W.M.; Rossen, J.W.A. Virulence factors of enteric pathogenic *Escherichia coli*: A Review. *Int. J. Mol. Sci.* **2021**, *22*, 9922. [CrossRef]
17. Rijo, P.; Falé, P.L.; Serralheiro, M.L.; Simões, M.F.; Gomes, A.; Reis, C. Optimization of medicinal plant extraction methods and their encapsulation through extrusion technology. *Measurement* **2014**, *58*, 249–255. [CrossRef]
18. Salazar-López, E.I.; Jimenez, M.; Salazar, R.; Azuara, E. Incorporation of Microcapsules in Pineapple Intercellular Tissue Using Osmotic Dehydration and Microencapsulation Method. *Food Bioprocess Technol.* **2015**, *8*, 1699–1706. [CrossRef]
19. Gallegos, G.; Lobato, G.; Gonzalez, C.; Herrera, R.; Zamilpa, A.; Álvarez, P. Preliminary phytochemical profile and bioactivity of *Inga jinicuil* Schltdl & Cham. ex G. Don. *Plants* **2022**, *11*, 794. [CrossRef]
20. Sánchez-Valdeolívar, C.A.; Álvarez-Fitz, P.; Zacapala-Gómez, A.E.; Mendoza-Catalán, M.A. Phytochemical profile and antiproliferative effect of *Ficus crocata* extracts on triple-negative breast cancer cells. *BMC Complement. Med. Ther.* **2020**, *20*, 191. [CrossRef]

21. Delgado, E.; Zamilpa, A.; González, M.; Olmedo, A.; Cardoso, A.; Sánchez, E.; Tapia, D.; Salinas, D.; Mendoza, P. Isorhamnetin: A nematocidal flavonoid from *Prosopis laevigata* leaves against *Haemonchus contortus* eggs and larvae. *Biomolecules* **2020**, *10*, 773. [CrossRef]
22. Li, Y.; Li, W.; Hu, D.; Lei, T.; Shen, P.; Li, J.; Gao, S. Metabolomics analysis reveals the role of cyanidin metabolism in *Plumbago auriculata* flower color. *Plant Biotechnol. Rep.* **2021**, *15*, 409–420. [CrossRef]
23. Lee, S.Y.; Ferdinand, V.; Siow, L.F. Effect of drying methods on yield, physicochemical properties, and total polyphenol content of chamomile extract powder. *Front. Pharmacol.* **2022**, *13*, 1003209. [CrossRef]
24. Clinical and Laboratory Standards Institute. *M100: Performance Standards for Antimicrobial Susceptibility Testing*, 34th ed.; Clinical and Laboratory Standards Institute: Wayne, PA, USA, 2024. Available online: https://webstore.ansi.org/standards/clsi/clsim100ed31?gad_source=1&gad_campaignid=1042641075&gbraid=0AAAAAD_gXFXMA-MD6r_935Mxd9PKSqhSD&gclid=Cj0KCQjwqqDFBhDhARIsAIHTlkum-0dNZVUCSmvdWYVyyg8oFqOhLjuPrbe_dGZMtAxT98vyCowqScwaAoOPEALw_wcB (accessed on 1 October 2025).
25. Hamzah, H.; Naeem, A.; Sabbar, M.; Ali, M.; Saleh, S.; Ali, H.; Majed, H. Effect of sub-MIC for Imipenem, Amikacin, and Cefixime on Growth and Swarming of *Proteus mirabilis*. *J. Pure Appl. Microbiol.* **2018**, *12*, 2241–2244. [CrossRef]
26. Panayi, T.; Sarigiannis, Y.; Mourelatou, E.; Hapeshis, E.; Papaneophytou, C. Anti-Quorum-sensing potential of ethanolic extracts of aromatic plants from the flora of Cyprus. *Plants* **2022**, *11*, 2632. [CrossRef]
27. Abascal, K.; Ganora, L.; Yarnell, E. The effect of freeze-drying and its implications for botanical medicine: A review. *Phytother. Res.* **2005**, *19*, 655–660. [CrossRef] [PubMed]
28. Ibarra, G.; Gutiérrez, M.; Robles, M.A. Análisis fitoquímico y actividad antibacteriana del extracto metanólico de hojas de *Plumbago auriculata* Lam. *Rev. Cienc. Biol. Salud* **2017**, *20*, 53–60. [CrossRef]
29. Ble, G.; Gómez, R.; Zamilpa, A.; López, R.; Lobato, G.; Álvarez, P. Ellagitannin, phenols, and flavonoids as antibacterials from *Acalypha arvensis* (Euphorbiaceae). *Plants* **2022**, *11*, 300. [CrossRef]
30. Zeng, L.; Chen, Y.; Liang, L.; Yang, L.; Wang, S.; Li, O.; Wang, Z. Comparison of different parts of *Plumbago zeylanica* L. through UPLC-MS/MS metabolite profiling and evaluation of their antioxidant and antifungal potential. *Pharmacol. Res. Nat. Prod.* **2024**, *5*, 100118. [CrossRef]
31. Hasan, M.; Hwija, I.; Mossa, Y. Essential oils from *Plumbago europaea* L. aerial parts (leaves, flowers): GC-MS analyses and literature biological properties. *Nat. Prod. Res.* **2023**, *39*, 341–350. [CrossRef]
32. Oikonomopoulou, V.; Krokida, M.; Karathanos, V. The influence of freeze-drying conditions on microstructural changes of food products. *Procedia Food Sci.* **2011**, *1*, 647–654. [CrossRef]
33. Kim, J.-W.; Taki, K.; Nagamine, S.; Ohshima, M. Preparation of poly (L-lactic acid) honeycomb monolith structure by unidirectional freezing and freeze-drying. *Chem. Eng. Sci.* **2008**, *63*, 3858–3863. [CrossRef]
34. Baibuch, S.; Zema, P.; Bonifazi, E.; Cabrera, G.; Mondragón Portocarrero, A.d.C.; Campos, C.; Malec, L. Effect of the drying method and optimization of extraction on antioxidant activity and phenolic content of rose Petals. *Antioxidants* **2023**, *12*, 681. [CrossRef]
35. Caliskan, G.; Dirim, S.N. The effect of different drying processes and the amounts of maltodextrin addition on the powder properties of sumac extract powders. *Powder Technol.* **2016**, *287*, 308–314. [CrossRef]
36. Saha, D.; Paul, S. Antibacterial activity of *Plumbago indica*. *Turk. J. Pharm. Sci.* **2014**, *11*, 217–222.
37. Rekha, S.R.; Kulandhaivel, M.; Hridhya, K.V. Eficacia antibacteriana y concentraciones inhibidoras mínimas de plantas medicinales contra patógenos de heridas. *Biomed. Pharmacol. J.* **2018**, *11*, 13–40. [CrossRef]
38. Khatun, A. *Plumbago indica* L.: A review of its medicinal uses, phytochemistry, pharmacology, and toxicology. *Int. J. Herb. Med.* **2023**, *11*, 31–37. [CrossRef]
39. Lou, Z.; Wang, H.; Rao, S.; Sun, J.; Ma, C.; Li, J. p-Coumaric acid kills bacteria through dual damage mechanisms. *Food Control* **2012**, *25*, 550–554. [CrossRef]
40. Sun, X.H.; Zhou, T.T.; Wei, C.H.; Lan, W.Q.; Zhao, Y.; Pan, Y.J.; Wu, V.C. Antibacterial effect and mechanism of anthocyanin rich Chinese wild blueberry extract on various foodborne pathogens. *Food Control* **2018**, *94*, 155–161. [CrossRef]
41. Guo, L.; Li, Y.; Feng, J.; Li, Y.; Liao, Y.; Zeng, Q.; Li, Y.; Yang, L.; Li, J.; Liu, C.; et al. Antibacterial activity and potential mechanisms of plumbagin against *Escherichia coli* and its application in milk. *Curr. Res. Food Sci.* **2025**, *10*, 101083. [CrossRef] [PubMed]
42. Shah, C.; Baral, R.; Bartaula, B.; Shrestha, L.B. Virulence factors of uropathogenic *Escherichia coli* (UPEC) and correlation with antimicrobial resistance. *BMC Microbiol.* **2019**, *19*, 204. [CrossRef]
43. Ford, K.M.; Antani, J.D.; Nagarajan, A.; Johnson, M.M.; Lele, P.P. Switching and torque generation in swarming *E. coli*. *Front. Microbiol.* **2018**, *9*, 2197. [CrossRef]
44. Norsworthy, A.; Pearson, M. From catheter to kidney Stone: The uropathogenic lifestyle of *Proteus mirabilis*. *Trends Microbiol.* **2017**, *25*, 304–315. [CrossRef]

45. Jamal, M.; Ahmad, W.; Andleeb, S.; Jalil, F.; Imran, M.; Nawaz, M.; Hussain, T.; Alí, M. Bacterial biofilm and associated infections. *J. Chin. Med. Assoc.* **2018**, *81*, 7–11. [CrossRef] [PubMed]
46. Alfhili, M.A.; Ahmad, I.; Alraey, Y.; Alangari, A.; Alqahtani, T.; Dera, A.A. Antibacterial and anti-biofilm activity of plumbagin against multidrug-resistant clinical bacterial isolates. *Saudi Med. J.* **2022**, *43*, 1224–1233. [CrossRef] [PubMed Central]

Disclaimer/Publisher's Note: The statements, opinions and data contained in all publications are solely those of the individual author(s) and contributor(s) and not of MDPI and/or the editor(s). MDPI and/or the editor(s) disclaim responsibility for any injury to people or property resulting from any ideas, methods, instructions or products referred to in the content.